

به نام خدا



دانشگاه صنعتی امیرکبیر
(پلی تکنیک تهران)

عنوان:

پروژه اول درس مدل سازی جریان های گردابی

استاد:

دکتر امانی

محمد رضا دانشور گرمودی

96126114

Part I:

Question 1: the Velocity profiles along x_2 have been plotted. As it can be seen in Fig. 1, if filter's width be smaller ($n=2$), the final results will be closer to DNS data. On the other hand, if filter's width be larger, the final results will be close to mean velocity. Also, near $y=0$, because the flow regime is mainly laminar, there is no fluctuation in there, so mean and filtered velocities are close to actual velocities. Moreover, if you notice, you will understand that the double filter with $n=2$ is very close to the single filter with $n=4$ but they are not exactly the same. The reason is that the filter's width is not the same in all nodes.

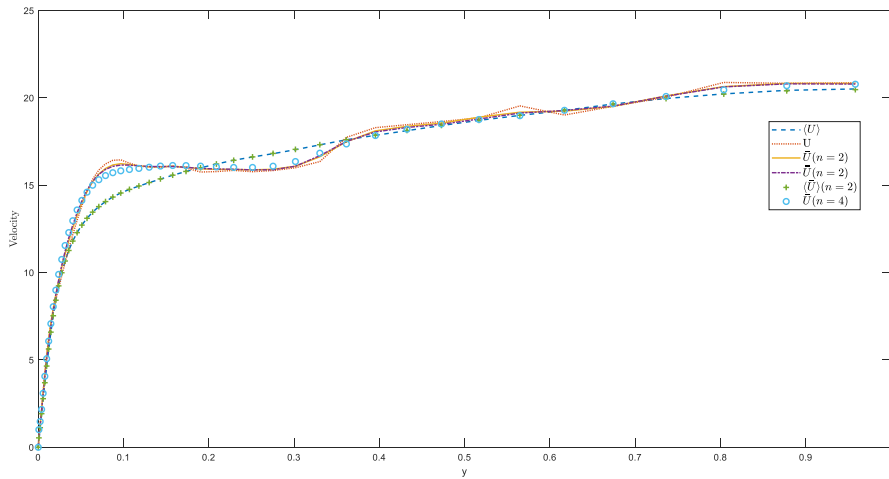


Fig. 1. Profile of velocities along x_2

Question 2: In Fig. 2, you can see that by taking the filter, we annihilate the fluctuations of the velocities. It depends on the width of the filter and by increasing the width, the profile will be smoother which you can see in Fig. 2. Moreover, if we take a filter with the width of all domain, the profile will be near zero, because filtering is a kind of averaging and the average of fluctuation parts will be zero.

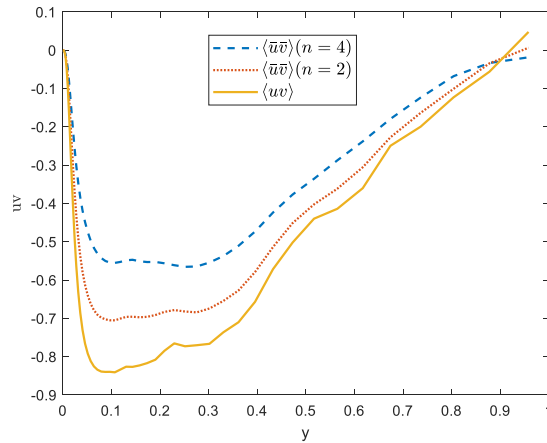


Fig. 2. Mean of Reynolds stress tensors along x_2

Question 3: From information in class, for simulation of turbulent flows, we need to model some terms. In RANS models, we should find proper models for Reynolds stress and for LES, we need to model $\tau_{i,j}^R$. Actually, the accuracy of the model depends on these two terms and they should be small in order to have an accurate model. In Fig. 3, we compared a specific component of these two terms. As it can be seen, in the smaller filter, $\tau_{1,2}^R$ is lower than the other ones. It is clear, because when the size of a filter is smaller, the model will be more accurate. Another important result is that, if we make the filter width bigger, $\tau_{1,2}^R$ will be close to Reynolds stress. That is because for Reynolds stress, we used mean of all domain, which means that if we take a filter with a width of near all domain, the results will be more like Reynolds stress.

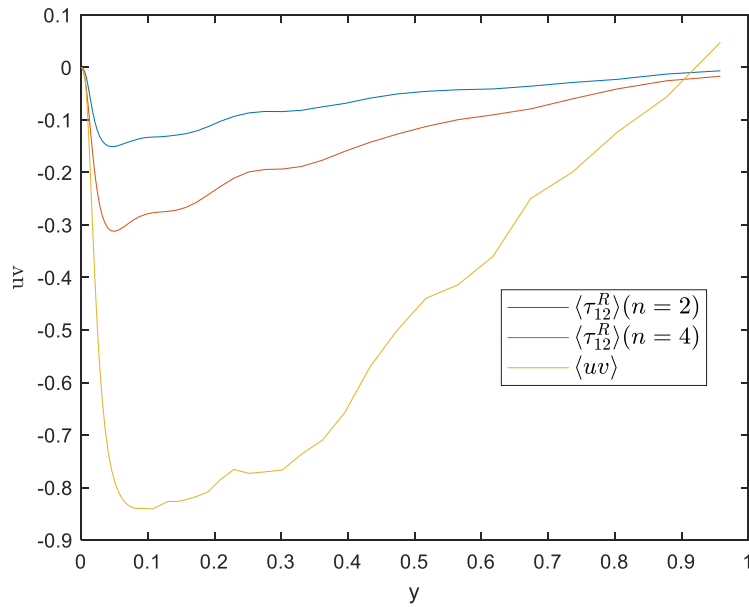


Fig. 3. Comparing residual-stress tensor and Reynolds stress tensor along x_2

Question 4: In this part, we have plotted a component of the mean of filtered shear rate tensor. As it can be seen in Fig. 4, near the wall ($y=0$), the magnitude of this component is so much higher than the middle of the channel. The reason is that the velocities have higher gradient near the wall and that is the reason why this component has higher value near the wall.

$$\bar{S}_{ij} = 0.5 \left(\frac{\partial \bar{U}_i}{\partial x_j} + \frac{\partial \bar{U}_j}{\partial x_i} \right)$$

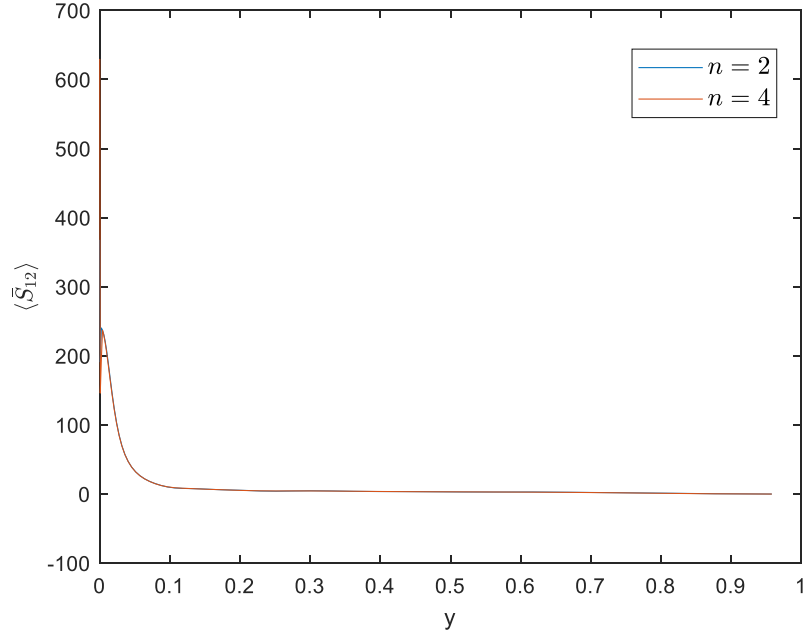


Fig. 4. Mean of filtered shear rate tensor along x_2

Part II

Question 1: In this part we investigated the accuracy of the Smagorinsky models:

$$\tau_{ij}^{R,M} - \frac{1}{3}\tau_{kk}^{R,M} = -2(C_s\Delta)^2 \bar{S}\bar{S}_{ij} \text{ (Static Model)}, \text{ Cs} = 0.05$$

$$\tau_{ij}^{R,M} - \frac{1}{3}\tau_{kk}^{R,M} = -2C_s(\Delta)^2 \bar{S}\bar{S}_{ij} \text{ (Dynamic Model)}, C_s = \frac{(M_{ij}L_{ij})_{ave}}{(M_{ij}M_{ij})_{ave}}$$

$$\bar{S} = (2\bar{S}_{ij}\bar{S}_{ij})^{0.5}$$

$$\text{Coefficient} = \frac{<\tau_{12}^R \tau_{12}^{R,M}>}{<\tau_{12}^R \tau_{12}^R>}$$

As it can be seen in Fig. 5, 6, Dynamic model can predict so much better than Static model, especially near the wall.

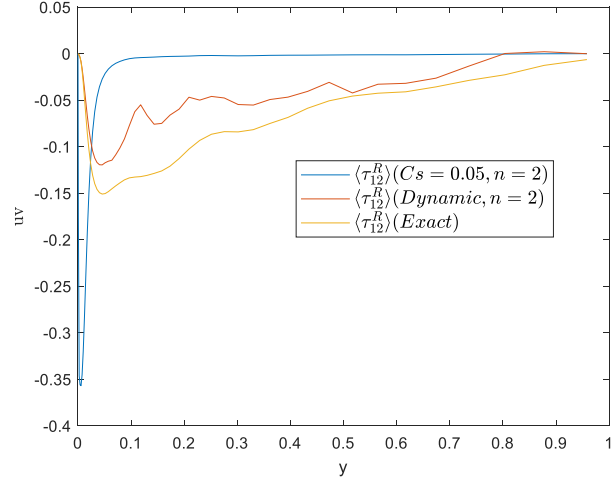


Fig. 5. Comparing different models with exact model along x_2

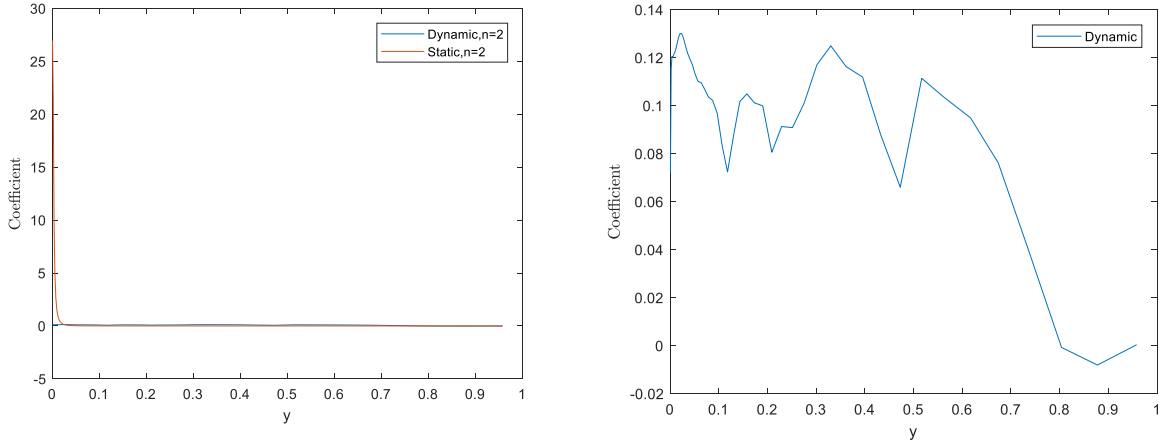


Fig. 6. Coefficient for different models along x_2

Question 2: In this part, we have compared $\frac{\nu_t}{\nu}$ for different models. This term can show us the intensity of turbulent in different parts of the domain. As you know, this parameter should be zero near walls, because that region is laminar. As it can be seen in Fig. 7 and 8, Dynamic model predict this behavior well but the Static model does not have this ability.

$$\nu_t = (Cs\Delta)^2 \bar{S} \quad (\text{Static Model}), \quad Cs = 0.05$$

$$\nu_t = Cs(\Delta)^2 \bar{S} \quad (\text{Dynamic Model}), \quad Cs = \frac{(M_{ij}l_{ij})_{ave}}{(M_{ij}M_{ij})_{ave}}$$

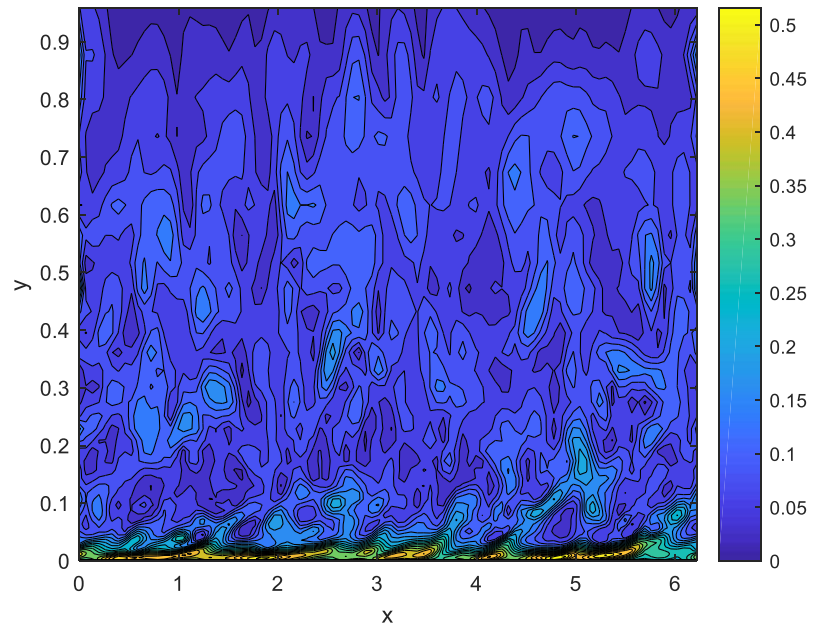


Fig. 7. contour of $\frac{\nu_t}{\nu}$ for Static model

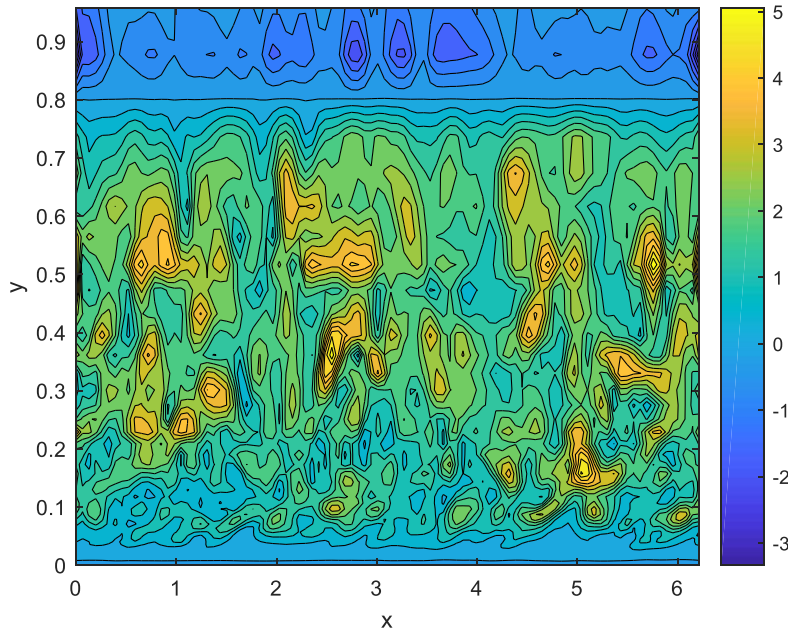


Fig. 8. contour of $\frac{\nu_t}{\nu}$ for Dynamic model

The reason why we have zero or negative $\frac{\nu_t}{\nu}$ for both Static and Dynamic models in the middle of the channel can be explained in this way that because there is no production in there (see Fig.11), we do not have so much turbulence in those regions.

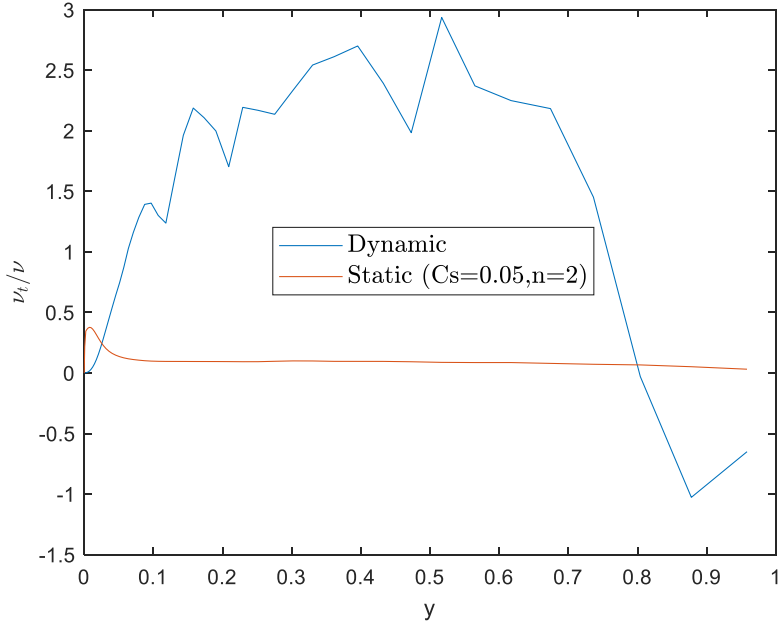


Fig. 9. Mean of $\frac{\nu_t}{\nu}$ for both Dynamic and Static ($n=2$) models along x_2

Question 3: in this section, we calculated the energy transfer rate for exact, dynamic, and static models. As it can be seen in Fig. 10, 11, and 12, near the wall we have energy production which is clear, because in that part, the energy will transfer from the mean flow. Also, you can see that exact and dynamic models are more close to each other but none of the dynamic and static models could get the backscatter which clearly exists in the exact result.

$$P_r = -\tau_{ij}^r \bar{S}_{ij}$$

$$P_r^M = -\tau_{ij}^{r,M} \bar{S}_{ij}$$

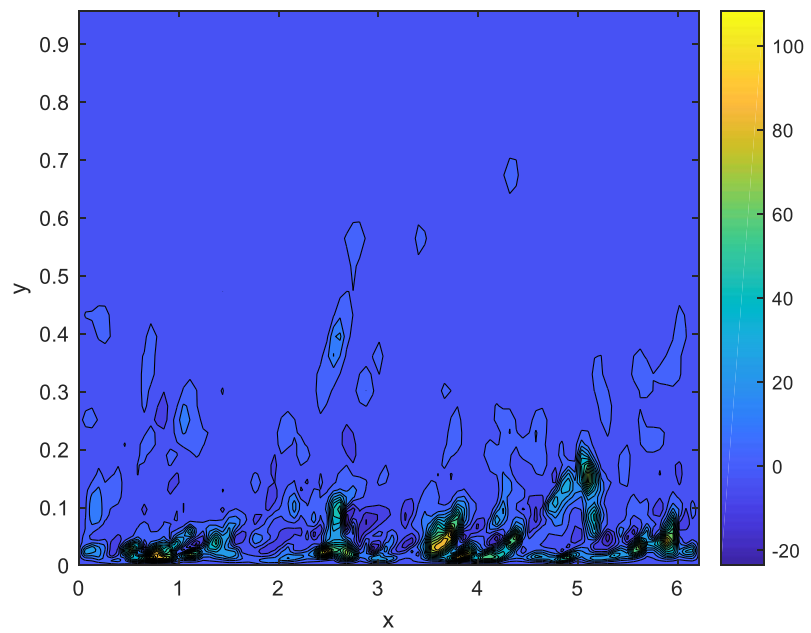


Fig. 10. contour of energy transfer rate for exact result

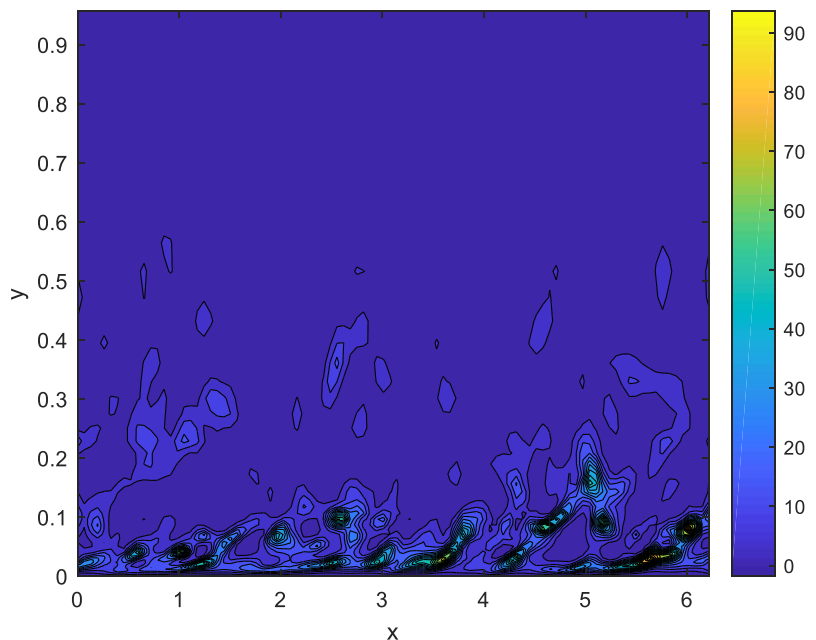


Fig. 11. contour of energy transfer rate for dynamic model

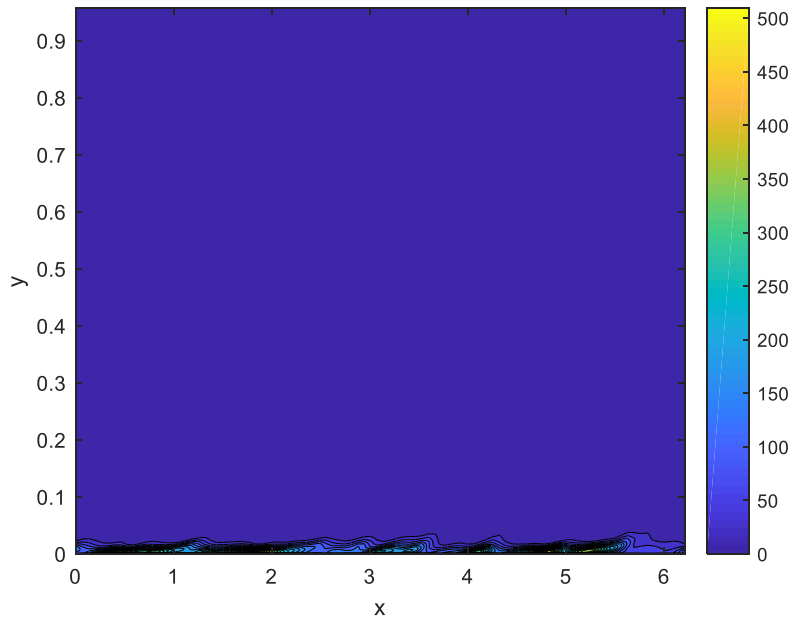


Fig. 12. Contour of energy transfer rate for Static model

Question 4: mean of energy transfer for different models have been plotted in Fig. 13. You can see that dynamic model is so much closer to exact results in comparison with the static model. However, we can find a proper C_s for the static model too, but it should change in different cases and also it can just tell us mean of energy transfer rate.

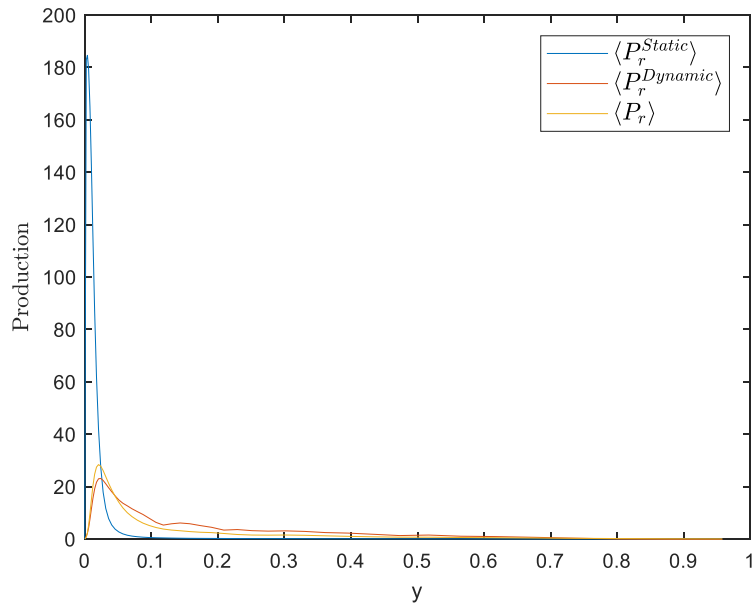


Fig. 13. Mean of energy transfer rate for different models along x_2

Question 5: In the last section, we have plotted $\frac{\langle \varepsilon_f \rangle}{\langle \varepsilon_r \rangle}$ and $\frac{\langle \varepsilon_r \rangle}{\langle P_r \rangle}$. Fig. 14 shows the ratio of

dissipation in resolved part on the dissipation in unresolved part. This should be high near wall, because in that region we have a higher gradient of velocity and if we take filter with smaller width, this will be even more, because it will be more accurate (more of dissipation will exist in resolved part and less in unresolved part). In the regions far from the wall, this will be lower which is shown in Fig. 14.

$$\varepsilon_f = 2\nu \bar{S}_{ij} \bar{S}_{ij}, \quad \varepsilon_r = \nu \left(\frac{\partial \bar{U}_l}{\partial x_j} \frac{\partial \bar{U}_l}{\partial x_j} - \frac{\partial \bar{U}_l}{\partial x_j} \frac{\partial \bar{U}_l}{\partial x_j} \right)$$

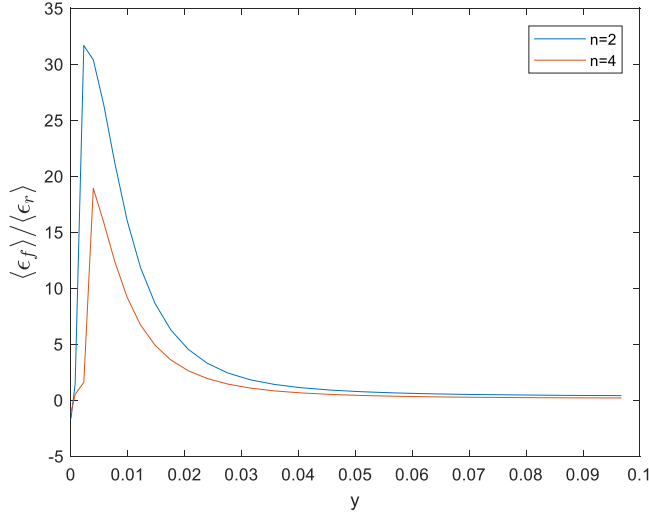


Fig. 14. Mean of the ratio of dissipation in resolved and unresolved parts along x_2

In Fig. 15, the ratio of dissipation in unresolved part on the energy which enters to unresolved part, has been plotted.

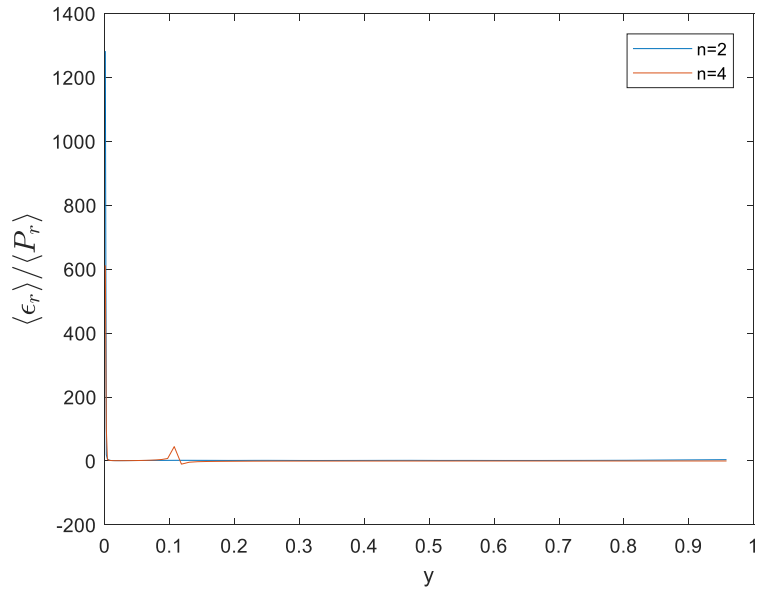


Fig. 15. Mean of the ratio of dissipation in unresolved part on the energy which enter to the unresolved part along x_2